Structure, magnetism and giant dielectric constant of $BiCr_{0.5}Mn_{0.5}O_3$ synthesized at high pressures

P. Mandal,[a] A. Iyo,[b] Y. Tanaka,[b] A. Sundaresan*[a] and C. N. R. Rao*[a]

Received 16th July 2009, Accepted 27th October 2009
First published as an Advance Article on the web 16th December 2009
DOI: 10.1039/b914350p

$BiCr_{0.5}Mn_{0.5}O_3$, synthesized at high pressure and high temperature, has a monoclinic structure (space group $C2/c$) at room temperature with $a = 9.4590(3)$ Å, $b = 5.5531(2)$ Å, $c = 9.6465(3)$ Å and $\beta = 108.149(2)^\circ$. It undergoes a structural transition from the monoclinic to an orthorhombic (Pnma) symmetry around 650 K. Magnetic measurements show three distinct anomalies at 25, 50 and 97 K. AC susceptibility measurements confirm the occurrence of the magnetic anomalies, but suggest no spin frustration. Interestingly, this oxide shows a giant dielectric constant at room temperature. Two clear relaxation processes commencing around 200 K and 300 K are exhibited by this material. The first relaxation process is due to Maxwell-Wagner polarization at the grain boundary whereas the second relaxation may arise from hopping of electrons in the B-site.

Introduction

There has been much interest in the study of bismuth-based transition metal oxides of the type $BiMO_3$ (M = 3d transition metal) possessing the perovskite structure because of their interesting multiferroic properties as well as structural features.[1–4] For example, La^{3+} and Bi^{3+} ions have similar ionic radii (1.16 Å and 1.17 Å in eight-fold coordination),[5] but $LaFeO_3$ crystallizes in a centrosymmetric orthorhombic structure (space group Pnma) while $BiFeO_3$ has a noncentrosymmetric rhombohedral structure (R3c).[6,7] The origin of the noncentrosymmetric distortion is attributed to the stereochemically active Bi^{3+} 6s lone pair electrons.[8] Thus, $BiFeO_3$ is multiferroic where the ferroelectricity ($T_{CE} \sim 1100$ K) originates from the Bi^{3+} ions and antiferromagnetism ($T_N \sim 650$ K) appears due to ordering of Fe^{3+} (S = 5/2) moments.[9] Among the $BiMO_3$ (M = transition metal) series, $BiMnO_3$ has been extensively studied recently with respect to the structure, magnetism and ferroelectric properties because it is the only material reported to be ferromagnetic with a T_C of 105 K.[3,10,11] Although ferroelectricity was initially reported in multiphasic sample of $BiMnO_3$,[12] later investigations of bulk samples as well as thin films have not confirmed ferroelectricity. Unlike $LaMnO_3$, which has the orthorhombic structure (Pnma), an early neutron diffraction study showed $BiMnO_3$ to possess a highly distorted noncentrosymmetric monoclinic structure (C2).[13] Recent studies based on convergent beam electron diffraction, however, show the presence of a centre of inversion.[14,15] Theoretical calculations suggest a centrosymmetric space group (C2/c) for ideal $BiMnO_3$.[16] Selected area electron diffraction studies have revealed the presence of a long-range ordered structure with C2 symmetry.[15] Oxygen nonstoichiometry has been reported to have a great influence on the structure and magnetism of $BiMnO_3$.[17,18] $BiCrO_3$ has a centrosymmetric monoclinic structure (C2/c) and undergoes a long range G-type antiferromagnetic ordering at $T_N = 109$ K with a weak ferromagnetic component.[19–21] The monoclinic angles of $BiMnO_3$ and $BiCrO_3$ differ, the values being 110.66° and 108.56° respectively.[14,21] It is worth noting that $BiScO_3$ is isostructural with $BiCrO_3$.[15,22] It, therefore, appears that the Bi^{3+} ion with the 6s lone pair does not always cause a noncentrosymmetric structure. It is noteworthy that except $BiFeO_3$, all the other bismuth-based $BiMO_3$ compounds (M = Sc, Cr, Mn, Co and Ni) require high pressures to stabilize them in the perovskite structure.

Bismuth-based oxides with two different magnetic ions at the B-site can show interesting magnetic properties due to various exchange couplings coming from their differing magnetic moments and symmetry of the orbital involved. For example, the ordered oxide, Bi_2NiMnO_6, is a ferromagnet with a high Curie temperature according to the Goodenough-Kanamori (GK) rules.[23] In Bi_2FeCrO_6, it was predicted that Fe^{3+} and Cr^{3+} order along the cubic (111) direction to give a rock-salt type ordering with a high ferrimagnetic transition temperature.[24] However, experimental results have shown that Fe and Cr ions are disordered at the B-site of the rhombohedral (R3c) structure with a collective magnetic ordering at 130 K likely to be due to frustration arising from Fe^{3+}–O–Fe^{3+}, Cr^{3+}–O–Cr^{3+} and Fe^{3+}–O–Cr^{3+} magnetic interactions.[25] In the present article, we report the structure, magnetism and dielectric properties of $BiCr_{0.5}Mn_{0.5}O_3$, prepared at high pressures. This combination of transition metals was chosen because certain oxidation states of Cr and Mn (Cr^{2+} and Mn^{4+}: d^4 and d^3) can be expected to exhibit a ferromagnetic ground state on ordering at the B-site. Contrary to this expectation, $BiCr_{0.5}Mn_{0.5}O_3$ is not an ordered compound and adopts the $BiCrO_3$ structure (C2/c) with a monoclinic angle of 108.140(2)°, undergoing a phase transition around 650 K. It exhibits a giant dielectric constant over a broad temperature and frequency range similar to $CaCu_3Ti_4O_{12}$ and related materials.

[a]*Chemistry and Physics of Materials Unit, Jawaharlal Nehru Centre for Advanced Scientific Research, Jakkur P.O., Bangalore, India 560064. E-mail: sundaresan@jncasr.ac.in; cnrrao@jncasr.ac.in*
[b]*Superconducting Materials Group, Nanoelectronic Research Institute, National Institute of Advanced Industrial Science and Technology (AIST), Tsukuba, Ibaraki, 305-8568, Japan*

Experimental

Polycrystalline $BiCr_{0.5}Mn_{0.5}O_3$ was synthesized under high pressure and high temperature employing a cubic anvil type apparatus. Stoichiometric amounts of preheated Bi_2O_3, Mn_2O_3 and Cr_2O_3 were mixed, ground well inside a glove box and pressed into a cylindrical shaped pellet. The pellet was placed inside a gold capsule and reacted at a temperature of 1073 K and a pressure of 4.5 GPa. Phase purity was confirmed using a Bruker D8 Advance X-ray diffractometer. A software package Fullprof was used to analyze the structural data and perform Rietveld refinement.[26] Differential scanning calorimetry data were collected on a Q2000 system (TA instruments). Magnetic properties were characterized by DC and AC susceptibility measurement in a Physical Property Measurement System (PPMS, Quantum Design, USA). Dielectric measurements were carried out with an Impedance Analyzer (Agilent 4294A) using compensated cable wire in a 4TP-2T configuration. Silver paint was used as electrode and the sample was placed in a custom made sample holder which goes inside the sample chamber of a 14 Tesla magnet cryo-cooled closed cycle refrigerator system. High temperature dielectric constant was measured by depositing gold on either side of the pellet and using a spring loaded sample holder.

Results and discussion

In Fig. 1, we show the X-ray diffraction (XRD) pattern of $BiCr_{0.5}Mn_{0.5}O_3$ subjected to Rietveld refinement based on the centrosymmetric (C2/c) monoclinic structure. The structural parameters of $BiCrO_3$ and $BiMnO_3$ were used as initial parameters for the refinement in space groups C2 and C2/c. The centrosymmetric space group C2/c was found to fit better than the non-centrosymmetric space group C2. The refined lattice parameters obtained from the Rietveld refinement are a = 9.4590(3) Å, b = 5.5531(2) Å, c = 9.6465(3) Å and β = 108.149(2)°. The observed monoclinic angle is very close to that reported for $BiCrO_3$. The other structural parameters such as atomic positions and isothermal factors are given in Table 1. Because of the presence of extra peaks due to unknown impurity phases the χ^2 value is higher but the parameters with standard errors are quite acceptable. As we could not identify the nature of the impurity phase, the extra peaks were excluded from the refinement. There are two crystallographic sites for the transition metals in the space group C2/c. Since it is difficult to determine the distribution of Cr and Mn ions over the two sites using laboratory X-rays, we distributed these ions equally among the two sites. Selected bond lengths and angles are given in Table 2. The Bi–O and average Cr/Mn–O bond lengths are comparable to those observed in $BiCrO_3$ and $BiMnO_3$. Bond valence sums calculated from the bond lengths are consistent with Bi^{3+}, Cr^{3+} and Mn^{3+} ions. This indicates that the transition metal ions are not ordered at the B-site as one would expect from the high stability of Cr(III) ions. The absence of long-range ordering of the transition metal ions is further supported by the magnetic properties where we do not see ferromagnetic ordering expected from the presence of Cr^{2+} (d^4) and Mn^{4+}(d^3) ions.

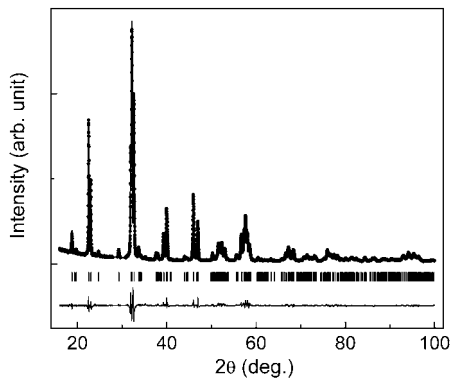

Fig. 1 Observed (dots) and calculated (line) X-ray diffraction pattern of $BiCr_{0.5}Mn_{0.5}O_3$ at room temperature. The bottom curve shows the difference pattern and the vertical marks are the symmetry allowed Bragg reflections.

High temperature X-ray diffraction data reveal the occurrence of a structural change from the monoclinic (C2/c) to an orthorhombic (Pnma) phase as shown in Fig. 2. The monoclinic-orthorhombic transition is complete at 873 K, but we observe the coexistence of the two phases in the 673 K and 773 K XRD patterns. At 673 K, a better fit was obtained for a mixture of C2/c and Pnma phases. Coexistence of the two phases indicates the first order nature of the phase transition. An endothermic peak at 650 K in differential scanning calorimetry (DSC) confirms the occurrence of the phase transition and its first-order nature. The DSC curves in Fig. 3 show the peaks at different temperatures while heating and cooling as expected of a first-order transition. Interestingly, the transition temperature of $BiCr_{0.5}Mn_{0.5}O_3$ is between those of $BiMnO_3$ (~770 K) and $BiCrO_3$ (~440 K).[3,19] At 873 K, the refined lattice parameters obtained by the profile fit for the Pnma space group are a = 5.5878(4) Å, b = 7.8606(7) Å and c = 5.4979(4) Å.

Fig. 4 shows the variation of the molar susceptibility under zero field-cooled (ZFC) and field-cooled (FC) conditions measured at 100 Oe. Three clear anomalies are seen at 25 K, 53 K and 96 K which disappear on applying a magnetic field of 10 kOe (see inset (a) in Fig. 4). Furthermore, the ZFC-FC curves coincide in the entire temperature range accompanied by a rise in susceptibility below 100 K. Above 100 K, the susceptibility follows Curie–Weiss behavior. The data were fitted to the Curie–Weiss law, $\chi = C/(T - \theta)$, where C is the Curie constant and θ is the Weiss temperature. From the fit, we obtain the effective magnetic moment μ_{eff} = 4.16 μ_B and the Weiss constant θ = 59 K. The value of μ_{eff} is closer to that expected for Cr^{3+} and Mn^{3+} ions. The Weiss constant for $BiCrO_3$ is negative (−359 K) whereas it is positive (126 K) for $BiMnO_3$ indicating the change in the nature of magnetic interaction from antiferromagnetic to ferromagnetic. The positive intermediate value of θ = 59 K in $BiCr_{0.5}Mn_{0.5}O_3$ is reasonable considering that both the end members have the same monoclinic structure.

The magnetic anomalies observed in $BiCr_{0.5}Mn_{0.5}O_3$ are similar to those reported for $BiCrO_3$ which shows three anomalies at slightly higher temperatures (40, 70 and 109 K) in the DC magnetization data.[20] The decrease in the magnetic transition temperatures in the former can arise due to the dilution of the Cr^{3+} ions in $BiCrO_3$ lattice with Mn^{3+} ions. As in the case of $BiCrO_3$, where the low-temperature anomaly at 40 K disappears upon applying high fields, all the three anomalies in

Table 1 Crystallographic data of $BiCr_{0.5}Mn_{0.5}O_3$ at room temperature

Atom	Wyckoff position	Oxidation	x	y	z	B_{iso}	Occ.
Bi	8f	+3	0.1328(1)	0.2172(2)	0.1287(2)	0.68(2)	0.952(3)
Cr1	4e	+3	0.0000	0.2303(8)	0.75	0.82(6)	0.25
Mn1	4e	+3	0.0000	0.2303(8)	0.75	0.82(6)	0.25
Cr2	4d	+3	0.25	0.25	0.50	0.82(6)	0.25
Mn2	4d	+3	0.25	0.25	0.50	0.82(6)	0.25
O1	8f	−2	0.089(1)	0.205(2)	0.584(1)	1.023	1.00
O2	8f	−2	0.149(2)	0.557(2)	0.378(2)	1.023	1.00
O3	8f	−2	0.351(2)	0.541(2)	0.164(1)	1.023	1.00

SG: C2/c, $a = 9.4662(3)$ Å; $b = 5.5577(2)$ Å; $c = 9.6538(4)$ Å; $b = 108.140(1)°$. $\chi^2 = 6.11$, $R_p = 10.6$, $R_{wp} = 11.7$, $R_{Bragg} = 4.88$, RF factor = 4.34.

Table 2 Selected bond lengths (Å), angles (°) and bond valence sums (BVS) of $BiCr_{0.5}Mn_{0.5}O_3$ at room temperature

Bi–O1	2.44(2), 2.40(2), 3.20(2)
Bi–O2	2.27(3), 2.80(3), 3.00(3)
Bi–O3	2.19(3), 2.68(2), 2.96(2), 3.22(3)
Cr1/Mn1–O1	2.03(2) ×2
Cr1/Mn1–O2	1.94(2) ×2
Cr1/Mn1–O3	2.06(2) ×2
Cr2/Mn2–O1	1.96(2) ×2
Cr2/Mn2–O2	2.13(2) ×2
Cr2/Mn2–O3	1.95(2) ×2
Cr1/Mn1–O1–Cr2/Mn2	152.8(9)
Cr1/Mn1–O2–Cr2/Mn2	161.8(10)
Cr1/Mn1–O3–Cr2/Mn2	149.6(9)
BVS Bi	2.90(1)
BVS Cr1/Cr2	2.94(7)
BVS Mn1/Mn2	3.23(8)

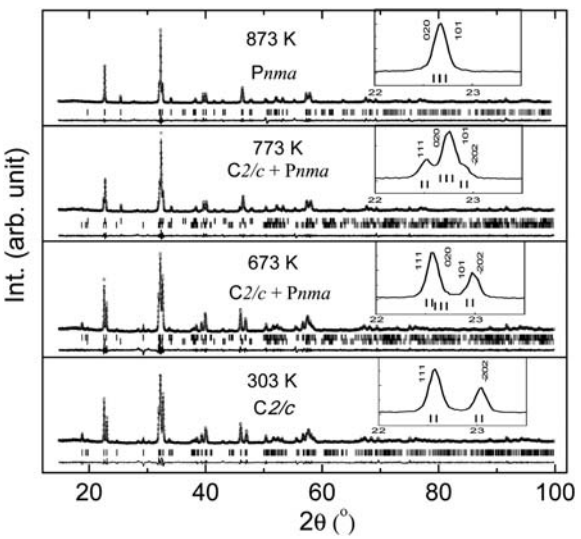

Fig. 2 X-Ray diffraction patterns at high temperatures showing monoclinic to orthorhombic transition.

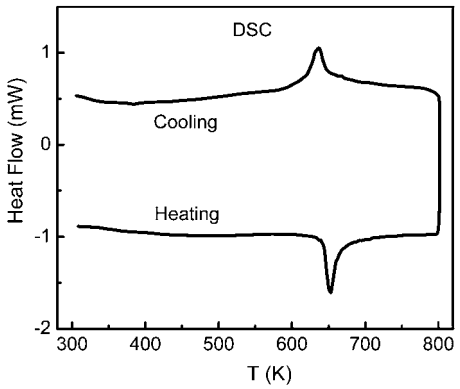

Fig. 3 Differential scanning calorimetry curves show that the monoclinic to orthorhombic transition is reversible.

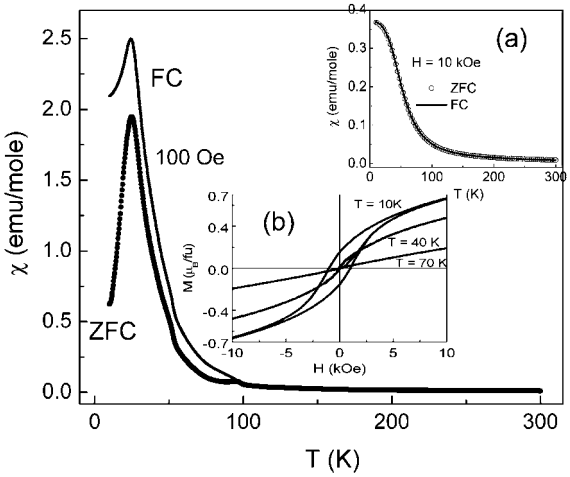

Fig. 4 Molar susceptibility *versus* temperature curves showing three anomalies at ca. 25, 50 and 97 K. The irreversibility between ZFC and FC curves below 97 K indicates the canting of magnetic moments. Inset (a) shows the temperature dependence of susceptibility at 10 kOe and (b) shows the magnetization *versus* field at various temperatures.

$BiCr_{0.5}Mn_{0.5}O_3$ disappear. Inset (b) in Fig. 4 shows the magnetic isotherms at 10, 40 and 70 K. At 10 K, the compound shows a hysteresis behavior without saturation indicating weak ferromagnetism at low temperatures. This is consistent with the fact that Cr^{3+} and Mn^{3+} ions are disordered at the B-site. The hysteresis becomes feeble with increase in temperature and becomes almost linear at 70 K.

AC susceptibility data of $BiCr_{0.5}Mn_{0.5}O_3$ were collected at different frequencies from 100 Hz to 10 kHz at an applied magnetic field of 5 Oe. The real and imaginary parts of the AC

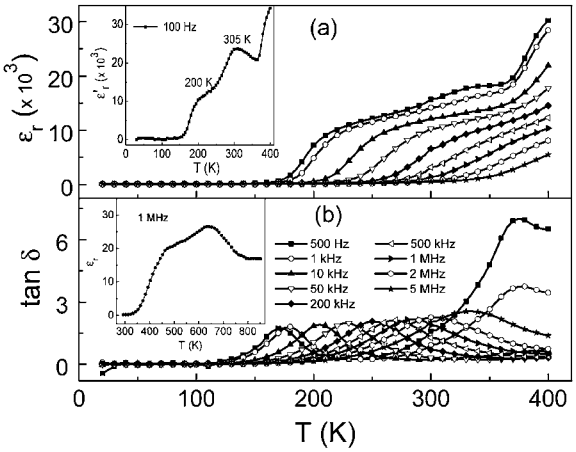

Fig. 5 Temperature dependence of (a) relative dielectric constant (ε_r), and (b) loss (tan δ) showing a giant dielectric constant at room temperature and two dielectric anomalies. Inset (a) shows two clear anomalies at low frequency (100 Hz) dielectric constant data. The dielectric anomaly at 650 K as shown in the inset of figure (b) is associated with the structural phase transition (see text).

susceptibility show three anomalies in agreement with the DC magnetization data. The real part χ' shows a small frequency dispersion below the first anomaly at 25 K whereas the imaginary part shows a frequency dispersion between the first and third anomalies. The absence of a shift in the peak positions with frequency indicates that the system is not a spin-glass.

Data on the variation of dielectric constant (ε_r) and loss tangent (tan δ) of $BiCr_{0.5}Mn_{0.5}O_3$ at different frequencies in the 20–400 K range (applied AC bias of 0.5 V) are shown in Fig. 5. The material exhibits a high dielectric constant (~14000 at 1 kHz) and loss (~0.95) at room temperature. Starting from a low value (~100), the dielectric constant increases rapidly above 200 K to high values (~10^4) with an anomaly around 300 K, the value increasing further up to 400 K as shown in Fig. 5a. The behavior is frequency-dependent and the peaks shift towards high temperatures with increasing frequency. The loss data in Fig. 5b show frequency-dependent peaks corresponding to the dielectric constant peaks. The loss peak due to the second anomaly occurs only at lower frequencies since it shifts towards higher temperatures at high frequencies. Interestingly, the loss peak appears for the first anomaly before the corresponding dielectric constant peak whereas it appears at a slightly higher temperature in the case of the second anomaly. Two relaxation processes seems to be associated with the dielectric anomalies below 400 K. This becomes evident from the dielectric constant data at 100 Hz shown as an inset in Fig. 5(a) and the loss data in Fig. 5b. The first dielectric anomaly may be related to Maxwell-Wagner relaxation due to the interfacial polarization at the grain boundaries. This phenomenon is common in a heterogeneous system where there is a difference between the grain and grain boundary conductivities due to which surface charges pile up at the interface, giving rise to a Debye-like relaxation on application of an AC bias.[27,28] As there is no structural transition around the second dielectric anomaly, we assign it to possible hopping of electrons among the transition metal ions. In addition to these two anomalies, the dielectric constant at high frequency (1 MHz) shows an anomaly near 640 K as shown in the inset of Fig. 5(b). This anomaly is related to the structural phase transition from the monoclinic to the orthorhombic phase, the shoulder around 450 K may correspond to the second anomaly observed in the low-temperature dielectric data. Dielectric and impedance measurements suggest the occurrence of Maxwell-Wagner relaxation at low temperatures and a contribution from grain boundaries to the dielectric properties, and detailed results of our analysis will be reported elsewhere.

Conclusions

$BiCr_{0.5}Mn_{0.5}O_3$ has been successfully prepared at high pressure and temperature. The material crystallizes in the centrosymmetric monoclinic structure (C2/c) similar to $BiCrO_3$. It undergoes a phase transformation to an orthorhombic phase (Pnma) around 640 K, but the transition is not associated with ferroelectric properties. Three distinct magnetic anomalies occur in the DC and AC susceptibility data in the 5–300 K range. The material exhibits a giant dielectric constant at room temperature and at least two dielectric anomalies below 400 K corresponding to Maxwell-Wagner relaxation and due to hopping of electrons among the transition metal ions.

Acknowledgements

The authors acknowledge TA instruments, Bangalore for DSC data and financial support from Department of Science and Technology (DST), Government of India, and Japan Science and Technology (JST), Japan, under the bilateral exchange program.

References

1 N. A. Hill, *J. Phys. Chem. B*, 2000, **104**, 6694.
2 J. Wang, J. B. Neaton, H. Zheng, V. Nagarajan, S. B. Ogale, B. Liu, D. Viehland, V. Vaithyanathan, D. G. Schlom, U. V. Waghmare, N. A. Spaldin, K. M. Rabe, M. Wuttig and R. Ramesh, *Science*, 2003, **299**, 1719.
3 T. Kimura, S. Kawamoto, I. Yamada, M. Azuma, M. Takano and Y. Tokura, *Phys. Rev. B: Condens. Matter Mater. Phys.*, 2003, **67**, 180401.
4 C. N. R. Rao and C. R. Serrao, *J. Mater. Chem.*, 2007, **17**, 4931.
5 R. D. Shannon, *Acta Crystallogr., Sect. A: Cryst. Phys., Diffr., Theor. Gen. Crystallogr.*, 1976, **32**, 751.
6 S. Geller and E. A. Wood, *Acta Crystallogr.*, 1956, **9**, 563.
7 F. Kubel and H. Schmid, *Acta Crystallogr., Sect. B: Struct. Sci.*, 1990, **46**, 698.
8 R. Seshadri and N. A. Hill, *Chem. Mater.*, 2001, **13**, 2892.
9 G. A. Smolenskii and I. E. Chupis, *Sov. Phys. Usp.*, 1982, **25**, 475.
10 F. Sugawara, S. Iiida, Y. Syono and S. Akimoto, *J. Phys. Soc. Jpn.*, 1968, **25**, 1553.
11 A. Moreira dos Santos, A. K. Cheetham, T. Atou, Y. Syono, Y. Yamaguchi, K. Ohoyama, H. Chiba and C. N. R. Rao, *Phys. Rev. B: Condens. Matter Mater. Phys.*, 2002, **66**, 064425.
12 A. Moreira dos Santos, S. Parashar, A. R. Raju, Y. S. Zhao, A. K. Cheetham and C. N. R. Rao, *Solid State Commun.*, 2002, **122**, 49.
13 T. Atou, H. Chiba, K. Ohoyama, Y. Yamaguchi and Y. Syono, *J. Solid State Chem.*, 1999, **145**, 639.
14 A. A. Belik, S. Iikubo, T. Yokosawa, K. Kodama, N. Igawa, S. Shamoto, M. Azuma, M. Takano, K. Kimoto, Y. Matsui and E. Takayama-Muromachi, *J. Am. Chem. Soc.*, 2007, **129**, 971.
15 T. Yokosawa, A. A. Belik, T. Asaka, K. Kimoto, E. Takayama-Muromachi and Y. Matsui, *Phys. Rev. B: Condens. Matter Mater. Phys.*, 2008, **77**, 024111.
16 P. Baettig, R. Seshadri and N. A. Spaldin, *J. Am. Chem. Soc.*, 2007, **129**, 9854.
17 A. Sundaresan, R. V. K. Mangalam, A. Iyo, Y. Tanaka and C. N. R. Rao, *J. Mater. Chem.*, 2008, **18**, 2191.

18 A. A. Belik, T. Kolodiazhnyi, K. Kosuda and E. Takayama-Muromachi, *J. Mater. Chem.*, 2009, **19**, 1593.
19 S. Niitaka, M. Azuma, M. Takano, E. Nishibori, M. Takata and M. Sakata, *Solid State Ionics*, 2004, **172**, 557.
20 A. A. Belik, N. Tsujii, H. Suzuki and E. Takayama-Muromachi, *Inorg. Chem.*, 2007, **46**, 8746.
21 A. A. Belik, S. Iikubo, K. Kodama, N. Igawa, S. Shamoto and E. Takayama-Muromachi, *Chem. Mater.*, 2008, **20**, 3765.
22 A. A. Belik, S. Iikubo, K. Kodama, N. Igawa, S. Shamoto, M. Maie, T. Nagai, Y. Matsui, S. Y. Stefanovich, B. I. Lazoryak and E. Takayama-Muromachi, *J. Am. Chem. Soc.*, 2006, **128**, 706.
23 M. Azuma, K. Takata, T. Saito, S. Ishiwata, Y. Shimakawa and M. Takano, *J. Am. Chem. Soc.*, 2005, **127**, 8889.
24 P. Baettig and N. A. Spaldin, *Appl. Phys. Lett.*, 2005, **86**, 012505.
25 M. R. Suchomel, C. I. Thomas, M. Allix, M. J. Rosseinsky, A. M. Fogg and M. F. Thomas, *Appl. Phys. Lett.*, 2007, **90**, 112909.
26 J. Rodríguez-Carvajal, abstracts of the Satellite Meeting on Powder Diffraction of the XV IUCr Congress, 1990, p. 127.
27 I. P. Raevski, S. A. Prosandeev, A. S. Bogatin, M. A. Malitskaya and L. Jastrabik, *J. Appl. Phys.*, 2003, **93**, 4130.
28 J. Liu, C. Duan, W. N. Mei, R. W. Smith and J. R. Hardy, *J. Appl. Phys.*, 2005, **98**, 093703.

